PCCP

COMMUNICATION

View Article Online
View Journal | View Issue

Cite this: *Phys. Chem. Chem. Phys.*, 2015, **17**, 32115

Received 7th September 2015,
Accepted 10th November 2015

DOI: 10.1039/c5cp05337d

www.rsc.org/pccp

Very fast bulk Li ion diffusivity in crystalline $Li_{1.5}Al_{0.5}Ti_{1.5}(PO_4)_3$ as seen using NMR relaxometry

Viktor Epp,*[ab] Qianli Ma,[c] Eva-Maria Hammer,†[c] Frank Tietz[cd] and Martin Wilkening*[ab]

The realization of large powerful all-solid-state batteries is still hampered by the availability of environmentally friendly and low-cost Li ion conductors that can easily be produced on a large scale and with high reproducibility. Advanced solid electrolytes benefit from fast ion-selective transport and non-flammability, but they may have low electrochemical stability with respect to Li metal. Sol–gel-synthesized lithium titanium aluminum phosphate $Li_{1.5}Al_{0.5}Ti_{1.5}(PO_4)_3$ (LATP), which was prepared *via* a new synthesis route taking advantage of an annealing step at relatively low temperatures, has the potential to become one of the major players in this field although it may suffer from reduction upon direct contact with metallic lithium. Its ion dynamics is, however, as yet poorly understood. In the present study, ^{7}Li nuclear magnetic resonance (NMR) spectroscopy was used to monitor the key Li jump processes on the atomic scale. NMR relaxation clearly reveals heterogeneous dynamics comprising distinct ultra-fast and slower diffusion processes. The high Li ion self-diffusion coefficients deduced originate from a rapid Li exchange with activation energies as low as 0.16 eV which means that sol–gel synthesized LATP is superior to other solid electrolytes. Our NMR results fully support recent theoretical investigations on the underlying diffusion mechanism, indicating that to rapidly jump from site to site, the ions use interstitial sites connected by low-energy barriers in LATP.

1. Introduction

It is hoped that the continuing demand for efficient electrochemical energy storage systems will be met, at least in the medium term, by rechargeable Li-based batteries that include, in particular, Li metal batteries with high energy densities.[1–7] Considering the conventional lithium-ion battery technology, great effort has been devoted to enhancing power, capacity, lifetime, and safety. Besides incremental improvements to existing systems, the availability of suitable solid electrolytes[8–13] is advantageous because of two considerations: (i) abandoning of highly flammable liquid electrolytes is expected to greatly improve safety and longevity, *i.e.*, to reduce aging processes; and (ii) the suppression of Li dendrite growth by making use of solid electrolytes working as both dense inorganic membranes and separators would allow the use of metallic Li as the anode material, instantly multiplying current energy densities. Moreover, fast solid ion-conductors may take over the same function in Li/sulfur batteries as well as in non-aqueous, and possibly even aqueous, Li/oxygen batteries.

Even without the use of Li anodes, all-solid-state batteries may be advantageous in (hybrid) automotive applications because they can easily withstand higher operation temperatures.[14] This also includes the use of industrial waste heat in stationary energy storage systems. Compared with the conductivity of liquid electrolytes, ion transport in solid electrolytes is often one order of magnitude slower and is regarded as one of the main drawbacks. Therefore, either thinner membranes or higher operation temperatures, *e.g.*, 80 °C, would be beneficial.

Research on solid electrolytes focuses on a wide range of materials including, in particular, various sulfides[15–20] and garnet-type oxides.[21–24] Although we have witnessed remarkable progress over the last few years, the optimum compound has not been found yet. Only a few materials have been identified whose ionic conductivities are on par with those of liquid electrolytes.[16,18–21,25–29] In our opinion, the renewed interest in Li-containing titanium aluminum phosphates (LATP) might boost research on solid Li ion electrolytes to a new level.[25,30–32]

To some extent, the present electrolytes suffer from the disadvantages of high-temperature synthesis routes, reproducibility issues concerning stoichiometry and defect chemistry, blocking grain boundaries, metastability, or even electrochemical instability. In contrast to garnet-type electrolytes, LATP-type compounds

[a] *Christian Doppler Laboratory for Lithium Batteries, and Institute for Chemistry and Technology of Materials, Graz University of Technology (NAWI Graz), Stremayrgasse 9, 8010 Graz, Austria. E-mail: viktor.epp@tugraz.at, wilkening@tugraz.at*
[b] *DFG Research Unit 1277, Mobility of Lithium Ions in Solids, Graz University of Technology, Austria*
[c] *Forschungszentrum Jülich GmbH, Institute of Energy and Climate Research, Materials Synthesis and Processing (IEK-1), 52425 Jülich, Germany*
[d] *Helmholtz-Institute Münster, c/o Forschungszentrum Jülich GmbH, 52425 Jülich, Germany*
† Present address: Ceres Power Ltd., Viking House, Foundry Lane, Horsham RH13 5PX, UK.

can be prepared more simply and with higher reproducibility because of the lower sintering temperatures needed (900 °C *vs.* temperatures higher than 1100 °C).[27] This directly prevents Li loss and ensures that the bulk and intra-grain properties are controlled more effectively. Combined with a high ionic conductivity, electrochemical robustness with respect to Li, *e.g.*, through the application of protection layers, and negligible electronic conductivity, LATP-based compounds are expected to perform best among the electrolytes studied so far. Apart from the conduction pathway, little is known, however, about the elementary steps of Li ion hopping, which govern bulk ion transport and which are the key properties of a powerful electrolyte. An elegant way to study slow and very fast bulk ion dynamics is provided by the use of Li nuclear magnetic resonance (NMR) spectroscopy, *i.e.*, by NMR line shape and relaxation measurements.[10,33,34] Since NMR is a contactless method, there is no need for special sample preparation; powder samples can be used that have been stored under an inert gas atmosphere, *i.e.*, fire-sealed in small glass ampoules.

In the present study, we chose $Li_{1+x}Al_xTi_{2-x}(PO_4)_3$ with $x = 0.5$ as one of the most promising compounds of the LATP family[25] to study bulk ion conductivity in depth. The sample with μm-sized crystallites was prepared by a novel sol–gel method that allowed us to control the composition and morphology of the product obtained (see below). Importantly, the low sintering temperatures prevent, in particular, Li loss during the final annealing step. Rhombohedral $Li_{1.5}Al_{0.5}Ti_{1.5}(PO_4)_3$ crystallizes with the space group $R\bar{3}c$. It is composed of alternating, corner-sharing $[PO_4]$ tetrahedra and $[TiO_6]$ octahedra, in which Li is reported to occupy mainly M1 sites (see Fig. 1) and to a lesser extent M3 sites.[35] In a recent neutron diffraction study it was found that in LATP, besides M1, Li ions occupy a position close to M2 but displaced towards *b*, therein denoted as M2′.[36] The replacement of Ti^{4+} by Al^{3+} ions needs extra Li ions for charge compensation and these ions occupy the interstitial voids.[29,37,38] This enhancement of the number of charge carriers directly affects Li ion dynamics.

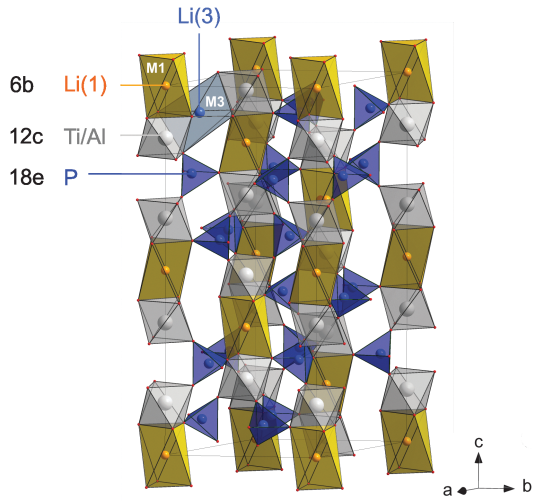

Fig. 1 Crystal structure of LATP-based electrolytes crystallizing with a rhombohedral lattice with a space group $R\bar{3}c$. The main site (M1) occupied by Li is shown by an orange polyhedron; in addition Li is reported to occupy the sites M3 to a much lower extent. Structural disorder and Li–Li interactions on the Li sublattice are expected to crucially influence Li ion dynamics. See the text for further details.

In the case of $Li_{1.5}Al_{0.5}Ti_{1.5}(PO_4)_3$ we found an exceptionally high Li ion diffusivity. NMR relaxometry (see below) revealed several diffusion-induced rate peaks that definitely point to complex ion dynamics. The very low activation energies deduced (0.16 eV), which we reliably assigned to Li ion translational motion, are in excellent agreement with those recently predicted theoretically.[39] The superposition of several diffusion processes gradually activated with increasing temperature results in an overall Li diffusivity that is in between those of Al-stabilized garnet oxides[21,23,24] and argyrodite-type sulfides.[40,41] The latter, together with the various compounds of the $Li_{10}GeP_2S_{12}$ group,[16,18] represent the fastest ion conductors studied over the past few years.[18,42] While sulfides are highly hygroscopic, garnet oxides may suffer from reproducibility problems with respect to purity, composition and morphology because of the higher annealing temperatures needed. In contrast, LATP-based electrolytes might be advantageous in terms of preparation and device fabrication.

2. Experimental

For the preparation of $Li_{1.5}Al_{0.5}Ti_{1.5}(PO_4)_3$ we developed a new sol–gel synthesis method. Stoichiometric amounts of $LiNO_3$ (99%, Alfa Aesar), $Al(NO_3)_3{\cdot}9H_2O$ (99%, Alfa Aesar), titanium(IV) isopropoxide (97%, Aldrich) and $NH_4H_2PO_4$ (99%, Merck) were used. Titanium(IV) isopropoxide (97%, Aldrich) was first added to deionized water immediately forming a precipitate of titanium hydroxide. The fresh precipitate was filtered, washed and dissolved in nitric acid (65%, Aldrich). When a clear TiO^{2+} nitrate solution was formed, a 2-fold molar amount of citric acid monohydrate (99%, Merck) was added to the solution to stabilize it. $LiNO_3$ and $Al(NO_3)_3{\cdot}9H_2O$ were then added to the TiO^{2+} nitrate solution while stirring. After the salts were dissolved, $NH_4H_2PO_4$ was added to the solution and a sol was immediately formed. Stirring was continued for another 0.5 h. After about 1 h, a stiff gel was spontaneously obtained. The gel was dried, calcined and milled in ethanol with zirconia balls on a milling bench. The ball-milled powder was put into a cylindrical pressing mold and pressed at a uniaxial pressure of 100 MPa. The pressed pellets were then sintered at 900 °C. White samples with a pure rhombohedral phase were obtained after sintering. The density of the pellets was over 95% of the theoretical density. More information can be found elsewhere.[43]

Bulk ion dynamics on the angstrom length scale was studied using various time-domain ^{7}Li NMR techniques including, in particular, variable-temperature spin-locking relaxometry. This allowed an unprecedented investigation of Li ion translational dynamics on different time and length scales. The measurements were conducted using an Avance III 300 solid-state NMR spectrometer connected to a 7 T cryomagnet (Bruker BioSpin); the nominal Larmor frequency $\omega_0/2\pi$ was 116 MHz. We used

the spin-lock technique and the saturation recovery technique to record longitudinal ($R_1 \equiv 1/T_1$) as well as transversal spin–lattice relaxation (SLR) rates ($R_{1\rho} \equiv 1/T_{1\rho}$) by applying short NMR excitation pulse lengths on the order of 2 μs. ^{7}Li NMR spectra were obtained *via* Fourier transformation of the free induction decays recorded by a single-pulse 90° experiment. At selected temperatures we recorded NMR echoes with the sequence 90°–t_e–64° (20 μs < t_e < 60 μs) to overcome receiver dead-time effects, *i.e.*, to capture sharply decaying components of the transient signals. While SLR NMR measurements in the laboratory frame are sensitive to ion dynamics of the order of the Larmor frequency, *i.e.*, in the 10^8 Hz range, those performed in the rotating frame at a locking frequency $\omega_1/2\pi$ of 30 kHz track diffusion parameters on the scale of 10^4 Hz. The SLR rates were obtained by fitting stretched exponentials to the corresponding magnetization transients. A more detailed description of the experimental setup can be found in earlier publications.[44–46] Additionally, preliminary impedance measurements were performed using the Concept 80 system (Novocontrol), providing a frequency range of 3 μHz to 20 MHz; for further details of the setup we also refer to earlier publications.[46–48]

3. Results and discussion

Our NMR line-shape analysis provides first insights into Li ion dynamics that can be made visible by averaging the dipolar magnetic and electric quadrupolar interactions. Recorded ^{7}Li NMR spectra are shown in Fig. 2a. At low temperatures they are composed of a dipolarly broadened NMR central line, which is best described by a Voigt profile, and a broad quadrupole component with a width of *ca.* 24 kHz at 185 K (see the corresponding echo spectrum in Fig. 2a). The line width of the central line decreases with increasing temperature due to the averaging of dipole–dipole interactions. Furthermore, at $T > 200$ K the broad quadrupole component has transformed into sharp satellite intensities; at 300 K the corresponding distinctly shaped powder pattern is fully developed. Since ^{7}Li is a spin-3/2 nucleus, the 90° singularities result from the interactions of the nuclear quadrupole moment with a non-vanishing electric field gradient (EFG) at the nuclear site. The appearance of an averaged powder pattern at higher T directly reveals rapid Li diffusivity. From the position of the singularities at 296 K, a quadrupole coupling constant of $C_Q(^7\text{Li}) \approx 45.4$ kHz can be deduced if we assume an averaged EFG with axial symmetry. The value of C_Q is to some extent dependent on T since various diffusion processes are activated stepwise with increasing temperature (see below). This behaviour is well known in the literature and belongs to the so-called 'universalities' in NMR line narrowing.[49,50] A complete averaging leading to vanishing satellite signals is only expected for materials with a sufficiently large number of electrically distinct Li sites, as is the case for amorphous materials.

Plotting the line width (full width at half maximum, FWHM) of the central NMR line as a function of T, Fig. 2b reveals that the onset of significant motional line narrowing is well below 140 K. In perfect agreement with this observation, the regime of extreme NMR line narrowing, determined by a line width of only 480 Hz, is already reached at temperatures as low as 200 K, *i.e.*, 100 K below room temperature. This value is similar to those observed for other fast ion conductors;[41,51] it does not change much even if we increase the temperature up to 500 K.

The onset of line narrowing at temperatures as low as 150 K clearly shows an impressively fast Li ion exchange among the magnetically different Li sites in LATP. Anticipating a rigid

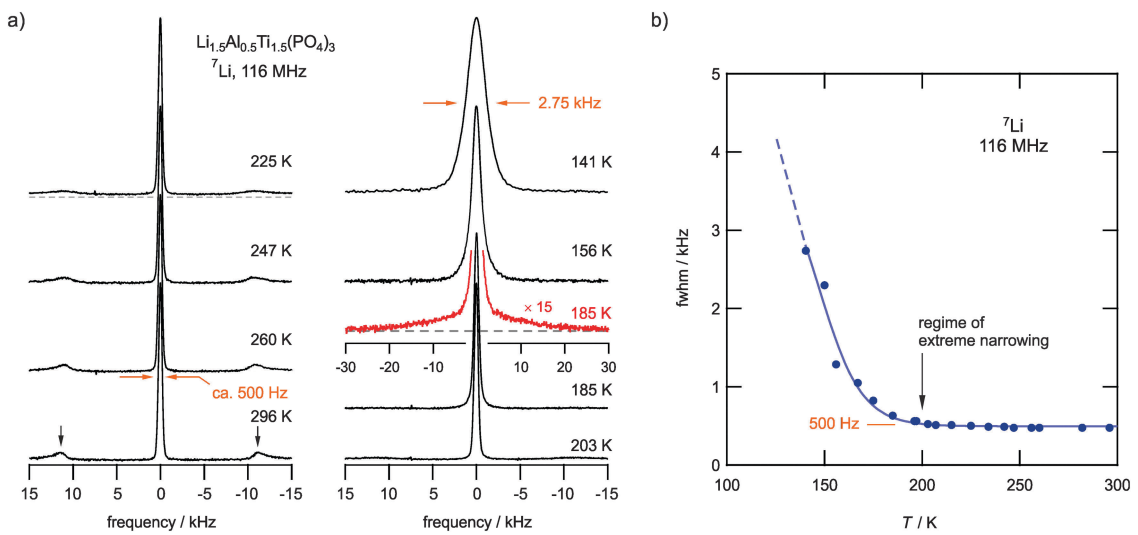

Fig. 2 (a) ^{7}Li NMR spectra of $Li_{1.5}Al_{0.5}Ti_{1.5}(PO_4)_3$ recorded by single-pulse experiments at 116 MHz; the temperatures are indicated. Even at temperatures as low as 220 K the averaged quadrupole powder pattern is seen that indicates extremely fast Li exchange processes, see, *e.g.*, the vertical arrows pointing to the 90° singularities of the spectrum recorded at 296 K. The spectrum recorded at 185 K (red line) was measured *via* the quadrupole echo technique; it reveals the quadrupole intensities at low T. (b) Line width (full width at half maximum, FWHM) of the NMR central transition as a function of temperature. The onset of motional narrowing, and thus the rigid lattice regime, is evidently well below 140 K. The regime of extreme narrowing is already reached at temperatures slightly below 200 K.

lattice line width of several kHz, full averaging is reached if the corresponding jump rate exceeds this value; thus, we have to deal with rates on the order of 10^4 s^{-1} at approximately 200 K.

The extraordinarily high Li diffusivity that leads to homonuclear dipole–dipole averaging is perfectly confirmed by the SLR NMR rates $R_{1(\rho)}$ recorded in both the laboratory and the rotating frame of reference.[52] We used the recorded SLR data to quantify the diffusion processes in terms of activation energies and diffusion coefficients.

In Fig. 3 the characteristic diffusion-induced rate peaks are displayed using an Arrhenius representation; the corresponding stretching exponents γ are also shown. While almost exponential transients were obtained in the case of R_1, γ of the transients in the rotating frame takes values of *ca.* 0.6 at low T. Most likely this is due to the coupling of the Li spins with paramagnetic centers as pointed out by Tse and Hartmann.[53] With increasing T, $\gamma(R_{1\rho})$ passes through a minimum that corresponds to the maxima in $R_{1\rho}$. This feature has also been observed for other Li ion conductors, see, *e.g.*, ref. 40. In the high-T limit the transients attain values of almost 1. This temperature behavior might point to heterogeneous dynamics, *i.e.*, spin reservoirs with distinct ion dynamics; further experiments are, however, needed to clarify the origins of the temperature dependence of the stretching exponents.

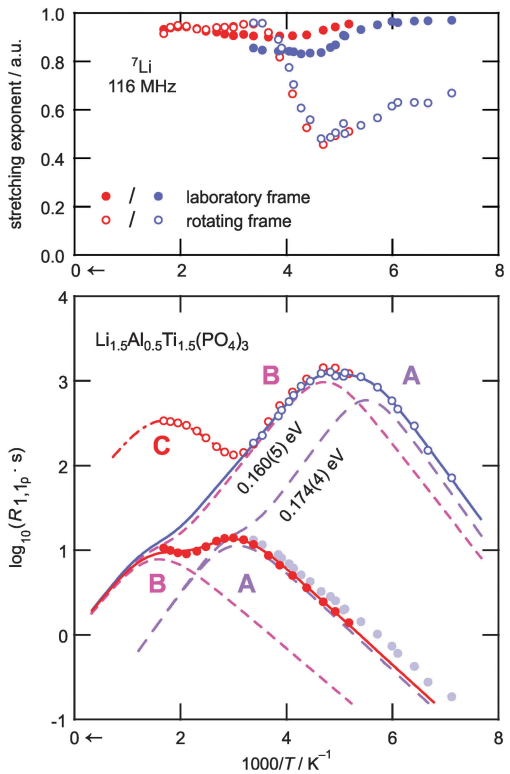

Fig. 3 (bottom) Arrhenius plot of the ^{7}Li NMR SLR rates R_1 and $R_{1\rho}$ of $Li_{1.5}Al_{0.5}Ti_{1.5}(PO_4)_3$ investigated in the laboratory (filled circles) and the rotating frame of reference (empty circles), respectively. The resonance frequency was $\omega_0/2\pi$ = 116 MHz. The red data points were recorded using a ceramic high-temperature probe, and the blue ones employing a cryoprobe. (top) Stretching exponents corresponding to the NMR SLR rates shown in the lower part of the figure. See the text for further discussion.

Coming back to the relaxation rate peaks shown in the lower part of Fig. 3, the jump rates at the temperatures of their maxima are on the order of 10^8 s^{-1} and 10^4 s^{-1} depending whether the measurements were performed in the laboratory frame or in the rotating frame. The data seem to suggest three distinct relaxation processes in the accessible temperature range, as evidenced by the number of maxima marked by A, B, and C in the figure. The process reflected by maximum C is only partially observable in the rotating frame at $T \geq 600$ K. The peak might reflect Li motion along a separate diffusion pathway that is activated at elevated temperatures only. Alternatively, it could represent rotational dynamics of the $[PO_4]$ or $[TiO_6]$ polyhedra. Further studies are needed to clarify this slow motion process. In contrast, the relaxation rate peaks A and B in both frames of reference are attributed to translational Li^+ hopping; they can be best described as a sum of two individual BPP-type expressions $R_1 = R_{1,A} + R_{1,B}$ and $R_{1\rho} = R_{1\rho,A} + R_{1\rho,B}$, respectively. According to NMR relaxation theory the proportionality of the summands is given by the following expressions:[54–56]

$$R_{1,\alpha} \propto J(\omega_0) + 4J(2\omega_0), \quad (1a)$$

$$R_{1\rho,\alpha} \propto 6J(2\omega_1) + 10J(\omega_0) + 4J(2\omega_0); (\alpha = A, B). \quad (1b)$$

For isotropic, random 3D jump relaxation processes, the underlying spectral density function $J(\omega)$ can be expressed by[56]

$$J(\omega) \propto \frac{\tau_c}{1 + (\omega\tau_c)^\beta}. \quad (2)$$

$\beta = 2$ results in symmetric relaxation peaks. Indeed, the data in the rotating frame of reference fulfill this behaviour and point to a quadratic frequency dependence. The spin–lattice relaxation rates in the laboratory frame, however, exhibit an asymmetry best described by a lower value for the parameter β. Here, β = 1.66 reproduces the lower slope of the low-temperature flank and accounts for correlation effects accessible in the timeframe of these experiments.

The correlation rate τ_c^{-1}, being the key parameter in this study, is of the order of the Li^+ jump rate; its temperature dependence is, in the simplest case, described using an Arrhenius relation

$$\tau_c^{-1} = \tau_0^{-1} \exp\left(-\frac{E_a}{k_B T}\right), \quad (3)$$

where E_a denotes the activation energy of the diffusion process, k_B Boltzmann's constant and τ_0^{-1} the pre-exponential factor.

At first glance, the following might be assumed: the peak pair A could be the result of dipolar Li spin relaxation in the immediate vicinity of paramagnetic centers, which would cause a relaxation shoulder of the main rate peak B. Such a behavior has been observed for several glasses by Müller-Warmuth and co-workers.[57] Since, however, a pronounced paramagnetic background relaxation is absent for the R_1 rates, we exclude this possibility of explaining the two rate peaks observed. Moreover, the corresponding R_1 rate peaks are well separated on the inverse temperature scale. Hence, we attribute the two observed peak maxima A and B to two dynamic processes that represent

distinct Li^+ elementary hopping processes in LATP. These processes could include jumps between M1 and M3 sites or also involve other interstitial sites. As pointed out by Lang *et al.*, incorporation of Al^{3+} causes the additional Li ions to occupy M3 sites.[39] At the same time Li^+ ions on M1 are displaced towards Al sites. This might result in a facile jump process as compared to Al-free LTP. As has been shown by Lang *et al.* the additional Li ions prefer to reside near the Al centers.[39] Such trapping effects would result in diffusion processes being activated at elevated T.

In order to extract the underlying diffusion parameters associated with the relaxation peaks, a global fit analysis was performed. Here, the rates R_1 and $R_{1\rho}$ are analyzed simultaneously, *i.e.*, by linking E_a and τ_0^{-1} that give rise to each peak. The resulting joint fits are shown as solid lines in Fig. 3 while the individual peak pairs are rendered as dashed lines. To be successful, it is necessary to formally replace the locking frequency ω_1 in the expression for $R_{1\rho,\alpha}$ by an effective frequency $\omega_{\mathrm{eff},\alpha}$, which takes into account local (magnetic and electric) fields. Since no information on these fields is available, $\omega_{\mathrm{eff},\alpha}$ was left as a free, *i.e.*, variable, parameter in the fit analysis. This results in virtually the same activation energies, *i.e.* $E_{a,A} = 0.17$ eV and $E_{a,B} = 0.16$ eV for both relaxation processes, while the pre-exponential factors of the Arrhenius terms turn out to be $\tau_{0,A}^{-1} \approx 3 \times 10^{11}\ s^{-1}$ and $\tau_{0,B}^{-1} \approx 1 \times 10^{10}\ s^{-1}$, respectively. The effective fields as obtained from the fits are $\omega_{\mathrm{eff,A}} \approx 2.1 \times 10^6\ s^{-1}$ ($\approx 11 \times \omega_1$) and $\omega_{\mathrm{eff,B}} \approx 8.6 \times 10^5\ s^{-1}$ ($\approx 4.6 \times \omega_1$).

Surprisingly, the determined activation energies are quite low. Similar values have recently been calculated for lithium titanium phosphate by Elsässer and co-workers on the basis of density functional theory: interstitial Li hopping (0.19–0.20 eV) is energetically preferred compared to vacancy-assisted migration.[39] Obviously, the interstitial diffusion mechanism suggested theoretically is confirmed experimentally by ^{7}Li NMR relaxometry.

The difference in pre-exponential factors $\tau_{0,A}^{-1}$ and $\tau_{0,B}^{-1}$ might be justified in different configurational entropies affecting the two diffusion processes. Depending on the exact diffusion pathway the ions may have access to a different number of available positions. Trapping effects because of Al centres (see above) may come into play, too. The different ω_{eff} values obtained might be the consequence of the site occupancy of paramagnetic impurities.

The diffusion parameters obtained by NMR can be used to calculate Li self-diffusion coefficients, which are the key parameters for the characterization of solid electrolytes. By employing the Einstein–Smoluchowski relation[58] and by assuming an uncorrelated jump diffusion with a mean diffusion length of about 3 Å, a value of $D \approx 3 \times 10^{-9}\ cm^2\ s^{-1}$ is obtained at room temperature (peak B). For peak A we obtain $D \approx 5 \times 10^{-8}\ cm^2\ s^{-1}$ at 300 K. Such a value corresponds to ionic conductivities on the order of 10^{-3} S cm^{-1}. This is observed by impedance spectroscopy: preliminary measurements of the bulk ion transport point to values of approx. 3×10^{-3} S cm^{-1} at 300 K. The corresponding activation energy of bulk ion transport amounts to 0.26 eV which is significantly lower than the mean values known for garnet-type oxides (0.34 eV), see below.[23]

Considering the activation energies from both NMR (0.16–0.17 eV, low T range) and impedance spectroscopy (0.26 eV) there are, at first glance, discrepancies, which can easily be understood in terms of a heterogeneous potential landscape to which the ions are exposed. In contrast to SLR NMR, which is sensitive to ion dynamics on the angstrom length scale, thus sensing activation barriers between next neighboring Li sites, impedance (or conductivity) spectroscopy probes long-range motions considering conductivities in the low-frequency range. The latter can be identified with DC values. Long-range ion transport through the crystal lattice is characterized by 0.26 eV, which is a mean value of all the barriers the ions have to overcome. Obviously, this also includes those which appear in SLR NMR at higher temperature, see peak C in Fig. 3.

Finally, we should compare the results of the NMR relaxometry responses with other fast-conducting solid electrolytes. Here, besides $Li_{10}GeP_2S_{12}$ and $Li_7P_3S_{11}$,[18,20] garnet-type cubic-$Li_{6.6}La_{0.3}Zr_{1.6}Ta_{0.4}O_{12}$ and argyrodite-type Li_6PS_5Br[41] serve as the boundaries of current research. Note, polycrystalline $Li_{6.6}La_3Zr_{1.6}Ta_{0.4}O_{12}$ was synthesized by a solid-state reaction using stoichiometric amounts of LiOH, La_2O_3, ZrO_2 and Ta_2O_5. After ball-milling in ethanol, the dried powder was pressed into pellets and calcined at 850 °C for 20 h in Al_2O_3 crucibles. Subsequent wet milling and sintering in pressed pellets was repeated first at 1000 °C, then at 1100 °C. The Arrhenius plot of Fig. 4 provides a succinct way to compare the diffusivities of the three samples *via* spin-lock NMR relaxometry. Since the rates shown were compared at similar locking frequencies, the position of the peak maxima directly reflects the extent of Li ion diffusivity. The more the peak is shifted towards lower temperatures the

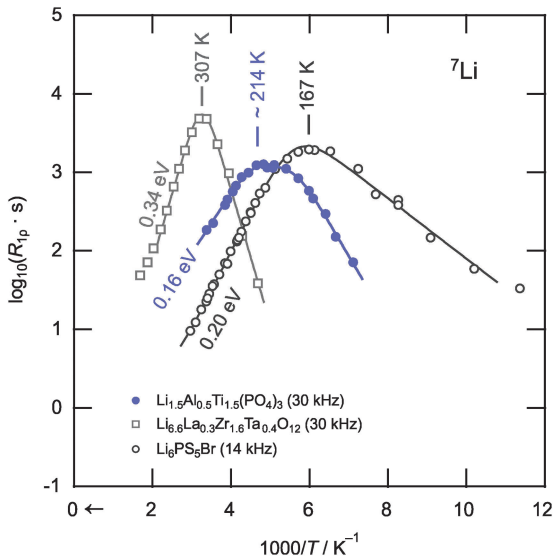

Fig. 4 Comparison of the ^{7}Li NMR SLR rates $R_{1\rho}$ shown in Fig. 2 with those obtained for $Li_{6.6}La_{0.3}Zr_{1.6}Ta_{0.4}O_{12}$ and Li_6PS_5Br,[41] representing members of two other promising candidates for solid electrolytes, *viz.* garnet-type oxides and structurally complex sulfides, respectively. The Li ion diffusivity as seen *via* NMR relaxometry clearly increases in the order $Li_{6.6}La_{0.3}Zr_{1.6}Ta_{0.4}O_{12}$ < $Li_{1.5}Al_{0.5}Ti_{1.5}(PO_4)_3$ < Li_6PS_5Br highlighting the extraordinary diffusion properties of LATP-based compounds.

higher is the Li ion mobility. Li_6PS_5Br can be identified as the compound with the highest Li-ion diffusivity (T_{max} = 167 K, 0.20 eV) and the garnet $Li_{6.6}La_{0.3}Zr_{1.6}Ta_{0.4}O_{12}$ that with the lowest (T_{max} = 307 K, 0.34 eV). The diffusivity of our LATP sample lies between the other two with respect to the relaxation process B (or even A). Hence, in terms of Li ion transport, the phosphate clearly shows superior properties as compared to oxide garnets.

4. Summary

To conclude, by making use of spin-lock and spin–lattice relaxation ^{7}Li NMR we were able to directly analyze bulk Li ion diffusivities in polycrystalline $Li_{1.5}Al_{0.5}Ti_{1.5}(PO_4)_3$ which is expected to be one of the next-generation solid electrolytes for Li-based batteries. The Li ion diffusivity in $Li_{1.5}Al_{0.5}Ti_{1.5}(PO_4)_3$ is extremely high and can easily compete with that of sulfide-based electrolytes, which, however, may suffer from hygroscopic properties that complicate both preparation and processing on a commercial level. ^{7}Li NMR relaxometry revealed several distinct diffusion processes pointing to a complex overall diffusion mechanism. The activation energies obtained (0.16–0.17 eV) are in excellent agreement with those recently calculated by Lang *et al.* (0.19 eV) for migrating interstitials in LATP.[39] This is one of the first important steps towards fully understanding the underlying ion transport mechanisms in lithium aluminium titanium phosphates.

Acknowledgements

We would like to thank our colleagues at TU Graz for valuable discussions. Financial support from the Austrian Federal Ministry of Science, Research and Economy, and the Austrian National Foundation for Research, Technology and Development is greatly appreciated. In addition, financial support from the Helmholtz Association in the framework of the project programs ''Helmholtz Energy Alliance – stationary electrochemical solid-state storage and conversion'' and ''HGF initiative for mobile/stationary energy storage systems'' is gratefully acknowledged. Moreover, we thank the Deutsche Forschungsgemeinschaft (DFG Research Unit 1277, grant no. WI3600/2-2 and 4-1) for financial support.

References

1 D. Larcher and J.-M. Tarascon, *Nat. Chem.*, 2015, **7**, 19.
2 P. G. Bruce, S. A. Freunberger, L. J. Hardwick and J.-M. Tarascon, *Nat. Mater.*, 2012, **11**, 19.
3 M. R. Palacin, *Chem. Soc. Rev.*, 2009, **38**, 2565.
4 P. G. Bruce, B. Scrosati and J.-M. Tarascon, *Angew. Chem., Int. Ed.*, 2008, **47**, 2930.
5 M. Armand and J.-M. Tarascon, *Nature*, 2008, **451**, 652.
6 M. S. Whittingham, *Chem. Rev.*, 2004, **104**, 4271.
7 J.-M. Tarascon and M. Armand, *Nature*, 2001, **414**, 359.
8 J. Sakamoto, in *Handbook Solid State Batteries*, ed. N. J. Dudney, W. C. West and J. Nanda, World Scientific, New Jersey, Hong Kong, 2015, p. 391.
9 Y. S. Jung, D. Y. Oh, Y. J. Nam and K. H. Park, *Isr. J. Chem.*, 2015, **55**, 472.
10 V. Epp and M. Wilkening, in *Handbook Solid State Batteries*, ed. N. J. Dudney, W. C. West and J. Nanda, World Scientific, New Jersey, Hong Kong, 2015, p. 133.
11 C. Cao, Z. Li, X.-L. Wang, X. Zhao and W.-Q. Han, *Front. Energy Res.*, 2014, **2**, 25.
12 K. Takada, *Acta Mater.*, 2013, **61**, 759.
13 P. Knauth, *Solid State Ionics*, 2009, **180**, 911.
14 M. Nagao, H. Kitaura, A. Hayashi and M. Tatsumisago, *J. Electrochem. Soc.*, 2013, **160**, A819.
15 G. Sahu, Z. Lin, J. Li, Z. Liu, N. Dudney and C. Liang, *Energy Environ. Sci.*, 2014, **7**, 1053.
16 P. Bron, S. Johansson, K. Zick, J. Schmedt auf der Günne, S. Dehnen and B. Roling, *J. Am. Chem. Soc.*, 2013, **135**, 15694.
17 T. Kaib, S. Haddadpour, M. Kapitein, P. Bron, C. Schröder, H. Eckert, B. Roling and S. Dehnen, *Chem. Mater.*, 2012, **24**, 2211.
18 N. Kamaya, K. Homma, Y. Yamakawa, M. Hirayama, R. Kanno, M. Yonemura, T. Kamiyama, Y. Kato, S. Hama, K. Kawamoto and A. Mitsui, *Nat. Mater.*, 2011, **10**, 682.
19 H.-J. Deiseroth, S.-T. Kong, H. Eckert, J. Vannahme, C. Reiner, T. Zaiß and M. Schlosser, *Angew. Chem., Int. Ed.*, 2008, **47**, 755.
20 F. Mizuno, A. Hayashi, K. Tadanaga and M. Tatsumisago, *Adv. Mater.*, 2005, **17**, 918.
21 V. Thangadurai, S. Narayanan and D. Pinzaru, *Chem. Soc. Rev.*, 2014, **43**, 4714.
22 J. Wolfenstine, J. Ratchford, E. Rangasamy, J. Sakamoto and J. L. Allen, *Mater. Chem. Phys.*, 2012, **134**, 571.
23 H. Buschmann, J. Dölle, S. Berendts, A. Kuhn, P. Bottke, M. Wilkening, P. Heitjans, A. Senyshyn, H. Ehrenberg, A. Lotnyk, V. Duppel, L. Kienle and J. Janek, *Phys. Chem. Chem. Phys.*, 2011, **13**, 19378.
24 R. Murugan, V. Thangadurai and W. Weppner, *Angew. Chem., Int. Ed.*, 2007, **46**, 7778.
25 K. Arbi, W. Bucheli, R. Jiménez and J. Sanz, *J. Eur. Ceram. Soc.*, 2015, **35**, 1477.
26 K. Takahashi, J. Ohmura, D. Im, D. J. Lee, T. Zhang, N. Imanishi, A. Hirano, M. B. Phillipps, Y. Takeda and O. Yamamoto, *J. Electrochem. Soc.*, 2012, **159**, A342.
27 J. L. Narváez-Semanate and A. C. M. Rodrigues, *Solid State Ionics*, 2010, **181**, 1197.
28 J. Fu, *Solid State Ionics*, 1997, **96**, 195.
29 H. Aono, E. Sugimoto, Y. Sadaoka, N. Imanaka and G. Adachi, *J. Electrochem. Soc.*, 1990, **137**, 1023.
30 E. C. Bucharsky, K. G. Schell, A. Hintennach and M. J. Hoffmann, *Solid State Ionics*, 2015, **274**, 77.
31 H. Morimoto, M. Hirukawa, A. Matsumoto, T. Kurahayashi, N. Ito and S. Tobishima, *Electrochemistry*, 2014, **82**, 870.
32 C. R. Mariappan, *Appl. Phys. A: Mater. Sci. Process.*, 2014, **117**, 847.
33 M. Wilkening and P. Heitjans, *ChemPhysChem*, 2012, **13**, 53.
34 R. Böhmer, K. R. Jeffrey and M. Vogel, *Prog. Nucl. Magn. Reson. Spectrosc.*, 2007, **50**, 87.
35 K. Arbi, S. Mandal, J. M. Rojo and J. Sanz, *Chem. Mater.*, 2002, **14**, 1091.

36 M. Pérez-Estébanez, J. Isasi-Marín, D. M. Többens, A. Rivera-Calzada and C. León, *Solid State Ionics*, 2014, **266**, 1.
37 P. Maldonado-Manso, E. R. Losilla, M. Martínez-Lara, M. A. G. Aranda, S. Bruque, F. E. Mouahid and M. Zahir, *Chem. Mater.*, 2003, **15**, 1879.
38 J. Fu, *J. Mater. Sci.*, 1998, **33**, 1549.
39 B. Lang, B. Ziebarth and C. Elsässer, *Chem. Mater.*, 2015, **27**, 5040.
40 V. Epp, Ö. Gün, H.-J. Deiseroth and M. Wilkening, *Phys. Chem. Chem. Phys.*, 2013, **15**, 7123.
41 V. Epp, Ö. Gün, H.-J. Deiseroth and M. Wilkening, *J. Phys. Chem. Lett.*, 2013, **4**, 2118.
42 A. Kuhn, V. Duppel and B. V Lotsch, *Energy Environ. Sci.*, 2013, **6**, 3548.
43 Q. Ma, F. Tietz and O. Guillon, 2015, submitted.
44 A. Dunst, V. Epp, I. Hanzu, S. A. Freunberger and M. Wilkening, *Energy Environ. Sci.*, 2014, **7**, 2739.
45 J. Langer, V. Epp, M. Sternad and M. Wilkening, *Solid State Ionics*, 2015, **276**, 56.
46 D. Wohlmuth, V. Epp and M. Wilkening, *ChemPhysChem*, 2015, **16**, 2582.
47 D. Wohlmuth, V. Epp, P. Bottke, I. Hanzu, B. Bitschnau, I. Letofsky-Papst, M. Kriechbaum, H. Amenitsch, F. Hofer and M. Wilkening, *J. Mater. Chem. A*, 2014, **2**, 20295.
48 F. Preishuber-Pflügl, P. Bottke, V. Pregartner, B. Bitschnau and M. Wilkening, *Phys. Chem. Chem. Phys.*, 2014, **16**, 9580.
49 R. Bertermann and W. Müller-Warmuth, *Z. Naturforsch., A: Phys. Sci.*, 1998, **53a**, 863.
50 A. Kuhn, P. Sreeraj, R. Pöttgen, H.-D. Wiemhöfer, M. Wilkening and P. Heitjans, *J. Am. Chem. Soc.*, 2011, **133**, 11018.
51 S. Narayanan, V. Epp, M. Wilkening and V. Thangadurai, *RSC Adv.*, 2012, **2**, 2553.
52 A. Kuhn, S. Narayanan, L. Spencer, G. R. Goward, V. Thangadurai and M. Wilkening, *Phys. Rev. B: Condens. Matter Mater. Phys.*, 2011, **83**, 94302.
53 D. Tse and S. R. Hartmann, *Phys. Rev. Lett.*, 1968, **21**, 511.
54 A. Abragam, *The Principles of Nuclear Magnetism*, Oxford University Press, Oxford, UK, 1961.
55 S. W. Kelly and C. A. Sholl, *J. Phys.: Condens. Matter*, 1992, **4**, 3317.
56 N. Bloembergen, E. M. Purcell and R. V Pound, *Phys. Rev.*, 1948, **73**, 679.
57 M. Grüne and W. Müller-Warmuth, *Solid State Nucl. Magn. Reson.*, 1995, **5**, 145.
58 H. Mehrer, *Diffusion in Solids: Fundamentals, Methods, Materials, Diffusion-Controlled Processes*, Springer, Berlin, New York, 2007.